

HPLC-ESIMSⁿ Profiling, Isolation, Structural Elucidation, and Evaluation of the Antioxidant Potential of Phenolics from *Paepalanthus geniculatus*

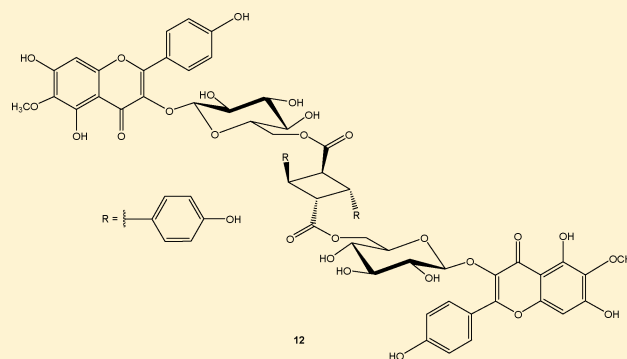
Fabiano Pereira do Amaral,[†] Assunta Napolitano,[‡] Milena Masullo,[‡] Lourdes Campaner dos Santos,[†] Michela Festa,[‡] Wagner Vilegas,[†] Cosimo Pizza,[‡] and Sonia Piacente^{*,‡}

[‡]Dipartimento di Scienze Farmaceutiche e Biomediche, Università degli Studi di Salerno, Via Ponte Don Melillo, 84084 Fisciano (SA), Italy

[†]Institute of Chemistry, Organic Chemistry Department, UNESP, São Paulo State University, CP 355, CEP 14800-900 Araraquara, São Paulo, Brazil

S Supporting Information

ABSTRACT: The methanol extract of the flowers of *Paepalanthus geniculatus* Kunth. showed radical-scavenging activity in the TEAC assay. An analytical approach based on HPLC-ESIMSⁿ was applied to obtain the metabolite profile of this extract and led to the rapid identification of 19 polyphenolic compounds comprising flavonoids and naphthopyranones. The new naphthopyranone (**10**, **16**), quercetagenin (**1**, **5**, **7**, **13**), and galetine derivatives (**9**, **11**, **17**, **19**), and a flavonol glucoside cyclodimer in the truxillate form (**12**), were identified. Compounds **2**, **6**, and **7** showed the highest antioxidant capacity and ability to affect the levels of intracellular ROS in human prostate cancer cells (PC3).



Paepalanthus, the largest genus of the Eriocaulaceae family, includes approximately 500 species distributed in Africa and Central and South America. Most of the known species grow in Brazil¹ and contain bioactive naphthopyranones and flavonoids.^{2–6} Glycosides of the naphthopyranone paepalantine are reported to exert a cytotoxic activity comparable to that of cisplatin⁷ and a lower mutagenic activity than paepalantine.⁸ Some naphthopyranones interfere with DNA repair systems,⁹ showing beneficial properties as potential anticancer drugs. Paepalantine displays antibiotic,¹⁰ mutagenic,¹¹ in vivo and in vitro cytotoxicity,¹² and intestinal anti-inflammatory effects.¹³

The remarkable antioxidant activity of paepalantine¹⁴ prompted us to evaluate the antioxidant capacity of the methanol extract of the flowers of *P. geniculatus* Kunth., a species not previously investigated.

The good antioxidant activity in the Trolox Equivalent Antioxidant Capacity (TEAC) assay^{15,16} (TEAC value = 1.479 mM) encouraged us to investigate its constituents. An analytical approach, based on HPLC-ESIMSⁿ, was applied to rapidly obtain a metabolite profile of the MeOH extract of the flowers of *P. geniculatus*. This guided the isolation of 19 polyphenolic compounds. The new compounds comprise two naphthopyranone (**10**, **16**), four quercetagenin (**1**, **5**, **7**, **13**), and four galetine derivatives (**9**, **11**, **17**, **19**) and one flavonol glucoside cyclodimer (**12**).

The antioxidant activities of the isolated metabolites were evaluated by the TEAC assay and by measuring the reduction

of the intracellular reactive oxygen species (ROS) levels in human prostate cancer cells (PC3) through flow cytometry.

RESULTS AND DISCUSSION

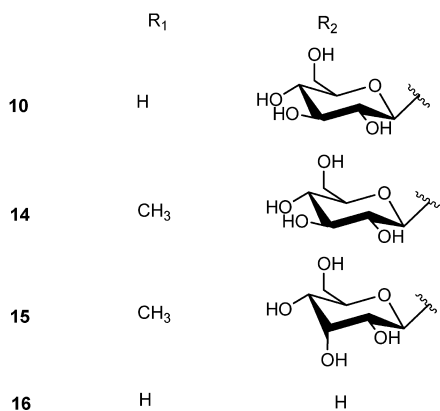
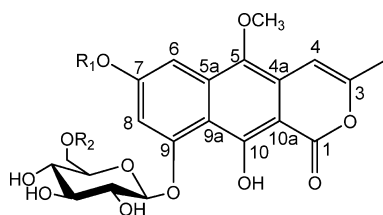
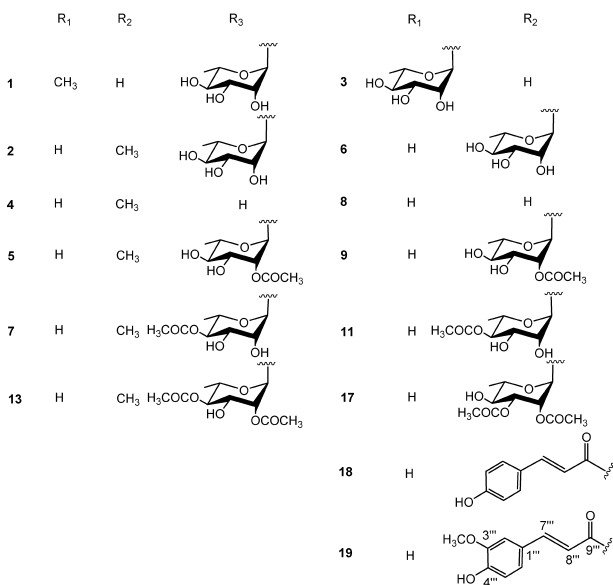
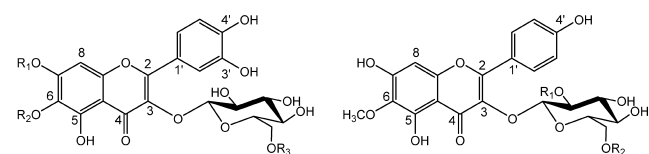
A preliminary metabolite fingerprint of the MeOH extract of the flowers of *P. geniculatus* was obtained by negative HPLC-ESIMSⁿ. Analysis of the ESIMSⁿ of the 19 compounds revealed the presence of glycosides of flavonoids (**1–9**, **11–13**, **17–19**) and naphthopyranones (**10**, **14–16**) (Supporting Information).

The MeOH extract was fractionated over Sephadex LH-20, and the fractions were rechromatographed by RP-HPLC-UV to yield compounds **1–19**. The known patuletin 3-*O*- β -D-rutinoside (**2**),¹⁷ 6-methoxykaempferol-3-*O*- α -L-rhamnopyranosyl-(1 \rightarrow 2)- β -D-glucopyranoside (**3**),¹⁸ patuletin 3-*O*- β -D-glucoside (**4**),¹⁷ 6-methoxykaempferol-3-*O*- α -L-rhamnopyranosyl-(1 \rightarrow 6)- β -D-glucopyranoside (**6**),¹⁹ 6-methoxykaempferol 3-*O*- β -D-glucoside (**8**),²⁰ paepalantine-9-*O*- α -D-glucopyranosyl-(1 \rightarrow 6)- α -D-glucopyranoside (**14**),⁴ paepalantine-9-*O*- β -D-allopyranosyl-(1 \rightarrow 6)- α -D-glucopyranoside (**15**),³ and 6-methoxykaempferol-3-*O*- β -D-6''-(*p*-coumaroyl)glucopyranoside (**18**)²¹ were identified by comparison of their observed and reported NMR and ESIMS data.

The positive HR-MALDI-TOFMS spectrum of **12** showed an $[M + H]^+$ ion at m/z 1249.3037, suggesting the molecular

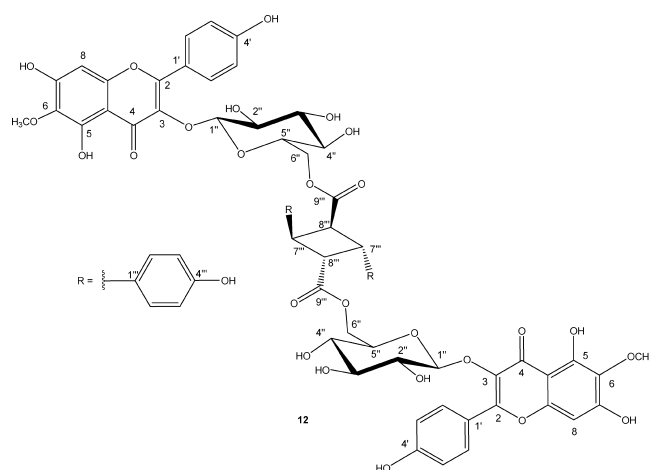
Received: July 19, 2011

Published: April 17, 2012



formula C₆₂H₅₆O₂₈ (calcd for C₆₂H₅₇O₂₈, 1249.3031). The ESIMS spectrum of **12** in the negative ion mode displayed an [M - H]⁻ ion at *m/z* 1247. The ESIMS² spectrum showed an ion [(M - 316) - H]⁻ at *m/z* 931, originating from the neutral loss of a galetine moiety, and a minor ion at *m/z* 623, due to loss of a 308 amu fragment. The ESIMS³ spectrum of the ion at *m/z* 623 yielded a major ion at *m/z* 315, due to the loss of a 308 amu fragment, thus suggesting a dimeric structure of **12** comprising two galetine units linked to a 308 amu moiety.

The ¹H NMR spectrum of compound **12** showed signals ascribable to *ortho*-coupled protons at δ 8.11 (2H, d, *J* = 8.6 Hz), 7.97 (2H, d, *J* = 8.5 Hz), 6.80 (2H, d, *J* = 8.6 Hz), and 6.76 (2H, d, *J* = 8.5 Hz), two singlets at δ 6.32 and 6.27, and



two signals at δ 3.87 and 3.83, corresponding to two methoxy groups (Table 1). Moreover, the ¹H NMR spectrum displayed two signals at δ 5.33 (d, *J* = 8.8 Hz) and 5.03 (d, *J* = 8.8 Hz), which, on the basis of 1D-TOCSY, DQF-COSY, HSQC, and HMBC experiments, were assigned to the anomeric protons of two β-glucopyranosyl units. A detailed analysis of the NMR data confirmed the presence of two 6-methoxykaempferol moieties. Significant downfield shifts of the C-6 methylene protons of the glucose units suggested that both C-6 hydroxy groups of the glucosyl units in **12** were acylated. The presence of a di(4-hydroxyphenyl)cyclobutanedicarboxylic lignan-type moiety was indicated by the aromatic proton signals at δ 6.60 (2H, d, *J* = 8.5 Hz), 6.56 (2H, d, *J* = 8.5 Hz), 6.85 (2H, d, *J* = 8.5 Hz), and 6.66 (2H, d, *J* = 8.5 Hz) and four methine proton signals at δ 4.07, 3.69, 3.47, and 3.44 (each ddd, *J* = 10.2, 8.6, 2.3 Hz) (Table 1). In the ¹³C NMR spectrum, signals due to the acyl moieties at δ 173.2 and 171.4 and four sp³ carbons at δ 48.5, 47.2, 41.9, and 40.9 were observed. The COSY experiment showed the sequence δ 4.07, 3.47, 3.69, 3.44, and this last signal correlated with the signal at δ 4.07, confirming the occurrence of a cyclobutane ring.²² The HSQC spectrum showed correlations between the proton signals at δ 4.07, 3.47, 3.69, and 3.44 and the corresponding carbons at δ 40.9, 48.5, 41.9, and 47.2, respectively. On this basis, the acyl units of **12** could be either truxinyl type ([7.7', 8.8']-lignan) or truxillyl type ([7.8', 8.7']-lignan).²³ HMBC correlations showed that the signals at δ 48.5 and 47.2 were attributable to the carboxyl-bearing carbons, while the signals at δ 41.9 and 40.9 were due to carbons linked to the 4-hydroxyphenyl moieties. In particular, correlations of the proton signal at δ 4.07 (H-7''') with the carbon resonance at δ 128.8 (H-2'''/H-6'''), the proton signal at δ 3.69 (H-7''') with the carbon resonance at δ 129.4 (H-2'''/H-6'''), and both protons at δ 4.07 and 3.69 with both carboxyl carbons at δ 173.2 and 171.4 suggested the placement of the acyl units as in a truxillyl derivative (Figure 1), as confirmed by the absence in the ROESY spectrum of correlations between the aromatic signals H-2'''/H-6''' of a 4-hydroxyphenyl group and H-2'''/H-6''' of the other 4-hydroxyphenyl group. The HMBC correlations of both H-7''' with both carboxylic carbons would not be expected in a truxinyl derivative (e.g., monochaetin in Figure 1). The orientation of the cyclobutane substituents was established by a ROESY experiment, which showed correlations of the equivalent H-2'''/H-6''' at δ 6.85 with both H-7''' and H-8''' at δ 3.47. Further correlations were observed between H-2'''/H-6''' (δ 6.60) and both H-7''' and H-8''' at δ 3.44. The presence

Table 1. ^{13}C and ^1H NMR Data (J in Hz) of Compounds **12** and **19** (600 MHz, δ ppm, in methanol- d_4)

	12		19	
	δ_{C}	δ_{H} (J in Hz)	δ_{C}	δ_{H} (J in Hz)
2	160.1		159.6	
3	133.6		135.5	
4	178.0		179.0	
5	150.0, 150.1		150.7	
6	131.0		132.5	
7	157.1		159.0	
8	94.9, 95.3	6.32, 6.27, s	95.5	6.47, s
9	152.0		153.4	
10	104.6		105.6	
1'	121.0		123.2	
2'	132.1, 131.9	8.11, d (8.6), 7.97 d (8.5)	131.9	8.03, d (8.5)
3'	115.8	6.80, d (8.6), 6.76, d (8.5)	116.0	6.85, d (8.5)
4'	157.1		161.3	
5'	115.8	6.80, d (8.6), 6.76, d (8.5)	116.0	6.85, d (8.5)
6'	132.1, 131.9	8.11, d (8.6), 7.97, d (8.5)	131.9	8.03, d (8.5)
OCH ₃ (C6)	60.7	3.87, 3.83, s	60.8	3.85, s
	β -D-Glc at C-3		β -D-Glc at C-3	
1''	103.1	5.33, d (8.8), 5.03, d (8.8)	103.5	5.26, d (8.8)
2''	75.4	3.54, dd (8.8, 9.0), 3.48, dd (8.8, 9.0)	75.5	3.49, dd (8.8, 9.0)
3''	77.4	3.46, dd (9.0, 9.0), 3.46, dd (9.0, 9.0)	77.8	3.47, dd (9.0, 9.0)
4''	71.5	3.15, dd (9.0, 9.0), 3.05, dd (9.0, 9.0)	71.5	3.37, dd (9.0, 9.0)
5''	76.1, 75.7	3.25, m, 2.75, m	75.5	3.47, m
6''	65.5, 64.5	3.95, dd (2.5, 12.0), 4.41, dd (2.5, 12.0), 3.79, dd (4.5, 12.0), 3.37, dd (4.5, 12.0)	63.8	4.31, dd (2.5, 12.0) 4.26, dd (4.5, 12.0)
	Truxillyl moiety		Acyl moiety	
1'''	114.6		127.5	
2'''	128.8, 129.4	6.60, d (8.5), 6.85, d (8.5)	111.5	7.10, d (1.9)
3'''	115.7	6.56, d (8.5), 6.66, d (8.5)	149.5	
4'''	156.9, 157.2		149.8	
5'''	115.7	6.56, d (8.5), 6.66, d (8.5)	116.3	6.84, d (8.5)
6'''	128.8, 129.4	6.60, d (8.5), 6.85, d (8.5)	123.5	6.94, dd (1.9, 8.5)
7'''	40.9, 41.9	4.07, ddd (10.2, 8.6, 2.3) 3.69, ddd (10.2, 8.6, 2.3)	114.5	6.15, d (16.0)
8'''	48.5, 47.2	3.47, ddd (10.2, 8.6, 2.3) 3.44, ddd, (10.2, 8.6, 2.3)	146.4	7.43, d (16.0)
9'''	173.2, 171.4		168.5	
OCH ₃ (C3''')			56.2	3.93, s

of the two 6-methoxykaempferolglucoside moieties and the probable puckering of the cyclobutane ring caused the upfield shift of the cyclobutane proton resonances, compared to those of the corresponding protons of a truxillate acid.²⁴ Moreover, the nonequivalence of NMR signals was due to the presence of the chiral glucose moieties, as previously reported for stachysetin, a dimer of apigenin-7-*O*-(6-*p*-coumaroyl)- β -D-glucopyranoside in the truxinate arrangement.²⁵

Geniculatin (**12**) represents a head-to-tail dimer of compound **18**, formed via photoinduced [2+2]-cycloaddition of two cinnamic acid moieties. Dimeric products including cyclobutane rings, produced from various phenylpropanoid acids, have been previously reported.²⁶ However, stachysetin from *Stachys aegyptiaca*²⁴ and monochaetin from *Monochaetum multiflorum*²⁶ are flavone glycoside dimers in the truxinate form (Figure 1). Thus, this is the first report of a diflavonoid ester of dicarboxylic acid in the truxillate arrangement.

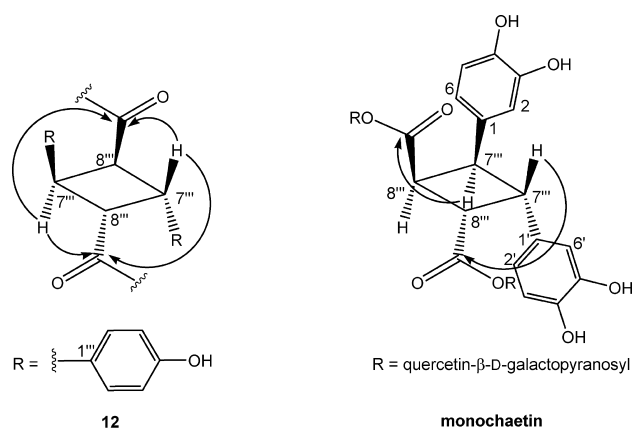
Compound **1** exhibited in the positive HR-MALDI-TOFMS spectrum an $[\text{M} + \text{H}]^+$ ion at m/z 641.1716, corresponding to the molecular formula $\text{C}_{28}\text{H}_{32}\text{O}_{17}$. The negative ESIMS spectrum displayed an $[\text{M} - \text{H}]^-$ ion at m/z 639. The

ESIMS² spectrum highlighted the presence of the aglycone ion at m/z 331, due to contemporary loss of two sugar units.

The ^1H NMR spectrum of compound **1** was similar to that of patuletin 3-*O*- β -D-rutinoside (**2**),¹⁷ except for the downfield shift of H-8 (δ 6.79) and the different chemical shift of the methoxy group (δ 4.02) (Table 2). On the basis of the correlation between the proton signal at δ 4.02 and the carbon resonance at δ 155.7 (C-7), the methoxy group was located at C-7. Thus compound **1** is the new 6-hydroxy-7-methoxyquercetin-3-*O*- α -L-rhamnopyranosyl-(1 \rightarrow 6)- β -D-glucopyranoside.

The positive HR-MALDI-TOFMS spectra of compounds **5** and **7** suggested the molecular formula $\text{C}_{30}\text{H}_{34}\text{O}_{18}$. The negative ESIMS spectra of the two compounds showed an $[\text{M} - \text{H}]^-$ ion at m/z 681. Analysis of the ESIMS² spectra of **5** and **7** showed the same fragmentation pattern and ascertained the presence of an acetyl moiety $\{[(\text{M} - 42) - \text{H}]^-, m/z$ 639}, a deoxyhexose $\{[(\text{M} - 42 - 146) - \text{H}]^-, m/z$ 493}, and a hexose $\{[(\text{M} - 42 - 146 - 162) - \text{H}]^-, m/z$ 331} moiety.

The ^1H NMR spectrum of compound **5** was similar to that of patuletin 3-*O*- β -D-rutinoside (**2**),¹⁷ except for the downfield shift observed for H-2_{tha} (δ 4.80) and an additional signal at δ



	12		monochaetin	
	δ_C	δ_H	δ_C	δ_H
7'''	40.9, 41.9	4.07	40.3, 40.1	3.89
		3.69		3.87
8'''	48.5, 47.2	3.47	46.2, 46.3	3.54
		3.44		3.46

Figure 1. Diagnostic HMBC correlations and ^{13}C and ^1H NMR data of the cyclobutane ring in the truxillate moiety (compounds 12) and in the truxinate moiety (monochaetin²⁶).

Table 2. ^{13}C and ^1H NMR Data (J in Hz) of the Aglycone Moieties of Compounds 1, 5, and 9 (600 MHz, δ ppm, in methanol- d_4)^a

	1		5		9	
	δ_C	δ_H (J in Hz)	δ_C	δ_H (J in Hz)	δ_C	δ_H (J in Hz)
2	159.7		159.7		159.4	
3	135.5		135.5		134.9	
4	179.0		179.0		179.4	
5	150.5		150.7		150.8	
6	131.4		132.4		132.7	
7	155.7		158.6		158.6	
8	91.3	6.79, s	95.0	6.55, s	95.0	6.56, s
9	151.3		153.8		153.6	
10	106.8		106.0		105.9	
1'	123.5		123.2		122.4	
2'	117.4	7.72, d (1.9)	117.4	7.68, d (1.9)	132.0	8.09, d (8.5)
3'	146.0		146.0		115.9	6.91, d (8.5)
4'	149.9		149.9		161.3	
5'	115.7	6.92, d (8.5)	115.8	6.91, d (8.5)	115.9	6.91, d (8.5)
6'	123.3	7.67, dd (1.9, 8.5)	123.5	7.66, dd (1.9, 8.5)	132.0	8.09, d (8.5)
OCH ₃ (C7)	56.5	4.02, s				
OCH ₃ (C6)			60.7	3.93, s	60.8	3.91, s

^aThe chemical shift values of the aglycone portion of 7 and 13 were superimposable with those reported for 5; the chemical shift values of the aglycone portion of 11 and 17 were superimposable with those reported for 9.

2.11 (s) corresponding to an acetyl function (Table 3). In the HMBC spectrum, correlations between the carbon resonance at δ 172.6 and the proton signals at δ 4.80 (H-2_{rha}) and 2.11 confirmed the presence of an acetyl group at C-2_{rha}. Thus, compound 5 is the new 6-methoxyquercetin-3-*O*-(2-*O*-acetyl)- α -L-rhamnopyranosyl-(1 \rightarrow 6)- β -D-glucopyranoside.

The NMR data of compound 7, in comparison with those of 5, suggested a different position of the acetyl group. In the COSY experiment, the downfield shifted signal at δ 4.82 was assigned to H-4_{rha} (Table 3). HMBC correlations between the carbon resonance at δ 172.8 and the proton signals at δ 4.82 (H-4_{rha}) and 2.04 confirmed the location of the acetyl function at C-4_{rha}. Thus, compound 7 is the new 6-methoxyquercetin-3-*O*-(4-*O*-acetyl)- α -L-rhamnopyranosyl-(1 \rightarrow 6)- β -D-glucopyranoside.

The molecular formula of compound 9 was established as C₃₀H₃₄O₁₇ by HR-MALDI-TOFMS (m/z 667.1874 [M + H]⁺, calcd for C₃₀H₃₅O₁₇, 667.1869). The ESIMS spectrum of compound 9 showed the [M - H]⁻ ion at m/z 665. The ESIMS² spectrum showed consecutive losses of 42, 146, and 162 amu, to afford the aglycone ion at m/z 315. The NMR data of the aglycone moiety of compound 9 (Table 2) were similar to those of 6,¹⁹ while the NMR data of the sugar region of 9 were closely related to those of 5, showing a 2-*O*-acetyl-rhamnopyranosyl unit linked to C-6 of the glucopyranosyl unit. Thus, compound 9 is the new 6-methoxykaempferol-3-*O*-(2-*O*-acetyl)- α -L-rhamnopyranosyl-(1 \rightarrow 6)- β -D-glucopyranoside.

HR-MALDI-TOFMS of 11 suggested the same molecular formula as 9. The NMR data of 11 were similar to those observed for 9, except for the ^1H and ^{13}C NMR values of the rhamnopyranosyl unit. In this case, H-4_{rha} (δ 4.82) instead of H-2_{rha} was downfield shifted due to the occurrence of the acetyl group at C-4_{rha}, as indicated by the HMBC correlation between the proton signal at δ 2.04 and the carbon resonance at δ 74.9 (C-4_{rha}). Thus, compound 11 is the new 6-methoxykaempferol-3-*O*-(4-*O*-acetyl)- α -L-rhamnopyranosyl-(1 \rightarrow 6)- β -D-glucopyranoside.

The HR-MALDI-TOFMS of 13 showed the [M + H]⁺ ion at m/z 725.1930 (calcd for C₃₂H₃₇O₁₉, 725.1924). The ESIMS² spectrum of the [M - H]⁻ ion at m/z 723 displayed an [(M - 42) - H]⁻ ion at m/z 681 whose ESIMS³ spectrum was similar to that of compound 5. The ^1H NMR spectrum of compound 13 was similar to that of 5 but showed a further signal at δ 2.04, corresponding to an acetyl group (Table 3). The ^1H NMR resonances of the sugar moiety in 13 differed from those of 5 in the downfield shift of H-4_{rha} (δ 4.74); this observation together with the HMBC correlation between the proton signal at δ 2.04 and the carbon resonance at δ 74.9 (C-4_{rha}) (Table 3) permitted the placement of a second acetyl group at C-4_{rha}. Thus, compound 13 is the new 6-methoxyquercetin-3-*O*-(2,4-di-*O*-acetyl)- α -L-rhamnopyranosyl-(1 \rightarrow 6)- β -D-glucopyranoside.

The HR-MALDI-TOFMS spectrum of 17 showed an [M + H]⁺ ion at m/z 709.1981, suggesting the molecular formula C₃₂H₃₆O₁₈ (calcd for C₃₂H₃₇O₁₈, 709.1974). The negative ESIMS spectrum displayed the [M - H]⁻ ion at m/z 707, 42 amu higher than those observed for 9 and 11, suggesting the occurrence of a further acetyl unit, as confirmed by ESIMSⁿ spectra. ^1H NMR data of 17 in comparison with those of 9 showed a further signal at δ 1.99, corresponding to an additional acetyl group (Table 3). COSY correlations between the anomeric proton of rhamnose at δ 4.52 with the signal at δ 5.02, which in turn correlated with the signal at δ 4.91,

Table 3. ^{13}C and ^1H NMR Data (J in Hz) of the Sugar Portions of Compounds **1**, **5**, **7**, **13**, and **17** (600 MHz, δ ppm, in methanol- d_4)^a

	1		5		7		13		17	
	δ_{C}	δ_{H} (J in Hz)	δ_{C}	δ_{H} (J in Hz)	δ_{C}	δ_{H} (J in Hz)	δ_{C}	δ_{H} (J in Hz)	δ_{C}	δ_{H} (J in Hz)
	β -D-Glc at C-3		β -D-Glc at C-3		β -D-Glc at C-3		β -D-Glc at C-3		β -D-Glc at C-3	
1	104.1	5.16, d (8.8)	104.3	5.14, d (8.8)	103.4	5.36, d (8.8)	103.3	5.36, d (8.8)	104.0	5.15, d (8.8)
2	75.3	3.51, dd (8.8, 9.0)	75.5	3.51, dd (8.8, 9.0)	75.4	3.54, dd (8.8, 9.0)	75.3	3.54, dd (8.8, 9.0)	75.4	3.49, dd (8.8, 9.0)
3	77.8	3.45, dd (9.0, 9.0)	78.0	3.44, dd (9.0, 9.0)	76.6	3.40, dd (9.0, 9.0)	76.9	3.40, dd (9.0, 9.0)	77.1	3.39, dd (9.0, 9.0)
4	71.8	3.30 dd (9.0, 9.0)	71.3	3.27 dd (9.0, 9.0)	70.9	3.41 dd (9.0, 9.0)	70.8	3.42 dd (9.0, 9.0)	71.3	3.25, dd (9.0, 9.0)
5	77.0	3.35 m	77.2	3.38 m	77.8	3.47 m	77.7	3.46 m	77.7	3.44, m
6	68.4	3.83, dd (2.5, 12.0)	68.6	3.88, dd (2.5, 12.0)	67.8	3.84, dd (2.5, 12.0)	68.0	3.82, dd (2.5, 12.0)	68.2	3.86, dd (2.5, 12.0)
		3.41, dd (4.5, 12.0)		3.40, dd (4.5, 12.0)		3.54, dd (4.5, 12.0)		3.60, dd (4.5, 12.0)		3.43, dd (4.5, 12.0)
	α -L-Rha at C-6 _{glc}		α -L-Rha at C-6 _{glc}		α -L-Rha at C-6 _{glc}		α -L-Rha at C-6 _{glc}		α -L-Rha at C-6 _{glc}	
1	102.0	4.54, d (1.2)	102.1	4.53, d (1.2)	101.8	4.60, d (1.2)	99.4	4.62, d (1.2)	99.1	4.52, d (1.2)
2	71.8	3.63, dd (1.2, 3.2)	75.5	4.80, dd (1.2, 3.2)	71.9	3.73, dd (1.2, 3.2)	73.7	4.97, dd (1.2, 3.2)	70.7	5.02, dd (1.2, 3.2)
3	71.8	3.56, dd (3.2, 9.7)	69.4	3.75, dd (3.2, 9.7)	70.0	3.72, dd (3.2, 9.7)	68.0	3.91, dd (3.2, 9.7)	72.7	4.91, dd (3.2, 9.7)
4	73.7	3.31, t (9.7)	70.7	3.50, t (9.7)	74.9	4.82, t (9.7)	74.9	4.74, t (9.7)	70.9	3.40, t (9.7)
5	69.4	3.46, m	69.5	3.58, m	67.2	3.60, m	67.5	3.62, m	69.5	3.60, m
6	17.6	1.14, d (6.5)	17.5	1.17, d (6.5)	17.4	0.90 d (6.5)	17.4	0.90, d (6.5)	17.7	1.17, d (6.5)
COOCH ₃ (C-2 _{rha})			172.6				170.5		171.9	
COOCH ₃ (C-2 _{rha})			20.9	2.11, s			20.6	2.09, s	20.5	2.06, s
COOCH ₃ (C-3 _{rha})									172.4	
COOCH ₃ (C-3 _{rha})									20.6	1.99, s
COOCH ₃ (C-4 _{rha})					172.8		171.0			
COOCH ₃ (C-4 _{rha})					20.8	2.04, s	20.7	2.04, s		

^aThe chemical shift values of the sugar portion of **9** and **11** were superimposable with those reported for **5** and **7**, respectively.

permitted location of the acetyl groups at C-2_{rha} and C-3_{rha} (Table 3). Thus, compound **17** is the new 6-methoxykaempferol-3-*O*-(2,3-di-*O*-acetyl)- α -L-rhamnopyranosyl-(1 \rightarrow 6)- β -D-glucopyranoside.

The HR-MALDI-TOFMS spectrum of **19** showed an $[M + H]^+$ ion at m/z 655.1663, supporting the molecular formula C₃₂H₃₀O₁₅ (calcd for C₃₂H₃₁O₁₅, 655.1657). The ESIMS spectrum of **19** showed the $[M - H]^-$ ion at m/z 653. The ESIMS² spectrum of this ion showed an ion at m/z 477 originating from the loss of a ferulic acid moiety (176 amu). The ^1H NMR spectrum of compound **19** showed two proton signals at δ 8.03 (d, $J = 8.5$, 2H) and 6.85 (d, $J = 8.5$, 2H), a singlet at δ 6.47 assigned to H-8, and a signal at δ 3.85, corresponding to a methoxy group (Table 1). These data, along with those derived from HSQC and HMBC experiments, allowed the identification of the aglycone moiety of **19** as 6-methoxykaempferol. Further signals occurring in the ^1H NMR spectrum at δ 7.10 ($J = 1.9$ Hz), 6.84 ($J = 8.5$ Hz), 6.94 ($J = 1.9$, 8.5 Hz), 6.15 ($J = 16.0$ Hz), 7.43 ($J = 16.0$ Hz), and 3.93 (3H, s) were attributed to an (*E*)-feruloyl moiety. This evidence, together with the occurrence of a β -glucopyranosyl unit, was confirmed by HSQC, HMBC, and COSY correlations. The downfield shifts of H₂-6 and C-6 of the glucose unit (δ_{H} 4.31 and 4.26; δ_{C} 63.8) suggested the location of the (*E*)-feruloyl moiety at C-6_{glc}. HMBC correlation between the two proton

signals at δ 4.31 and 4.26 with the carboxylic carbon at δ 168.5 confirmed this assumption. Thus, compound **19** is the new 6-methoxykaempferol-3-*O*-(6-*E*-feruloyl)- β -D-glucopyranoside.

The positive HR-MALDI-TOFMS spectrum of compound **10** showed an $[M + H]^+$ ion at m/z 613.1770, corresponding to the molecular formula C₂₇H₃₂O₁₆. The tandem ESIMS spectrum of the $[M - H]^-$ ion at m/z 611 showed two ions at m/z 449 and 287, originating from the consecutive losses of 162 amu. The fragmentation pattern of the ion at m/z 287 suggested a naphthopyranone structure (Figure 2).

The NMR data of **10** were similar to that of paepalantine-9-*O*- α -D-glucopyranosyl-(1 \rightarrow 6)- α -D-glucopyranoside (**14**),⁴ differing in the absence of the methoxy group at C-7 (Table 4). Consequently, compound **10** is the new 7,9,10-trihydroxy-5-methoxy-3-methyl-1*H*-naphtho[2,3-*c*]pyran-1-one-9-*O*- β -D-glucopyranosyl-(1 \rightarrow 6)- β -D-glucopyranoside.

The HR-MALDI-TOFMS spectrum of **16** showed an $[M + H]^+$ ion at m/z 451.1239, suggesting the molecular formula C₂₁H₂₂O₁₁ (calcd for C₂₁H₂₃O₁₁, 451.1235). The full negative mass spectrum of **16** displayed an $[M - H]^-$ ion at m/z 449. The ESIMS² spectrum showed an $[(M - 162) - H]^-$ ion at m/z 287, and multistage mass spectra of this ion indicated its naphthopyranone nature.

The ^1H NMR spectrum of the aglycone moiety of compound **16** was similar to that of **10**, but in the sugar region showed

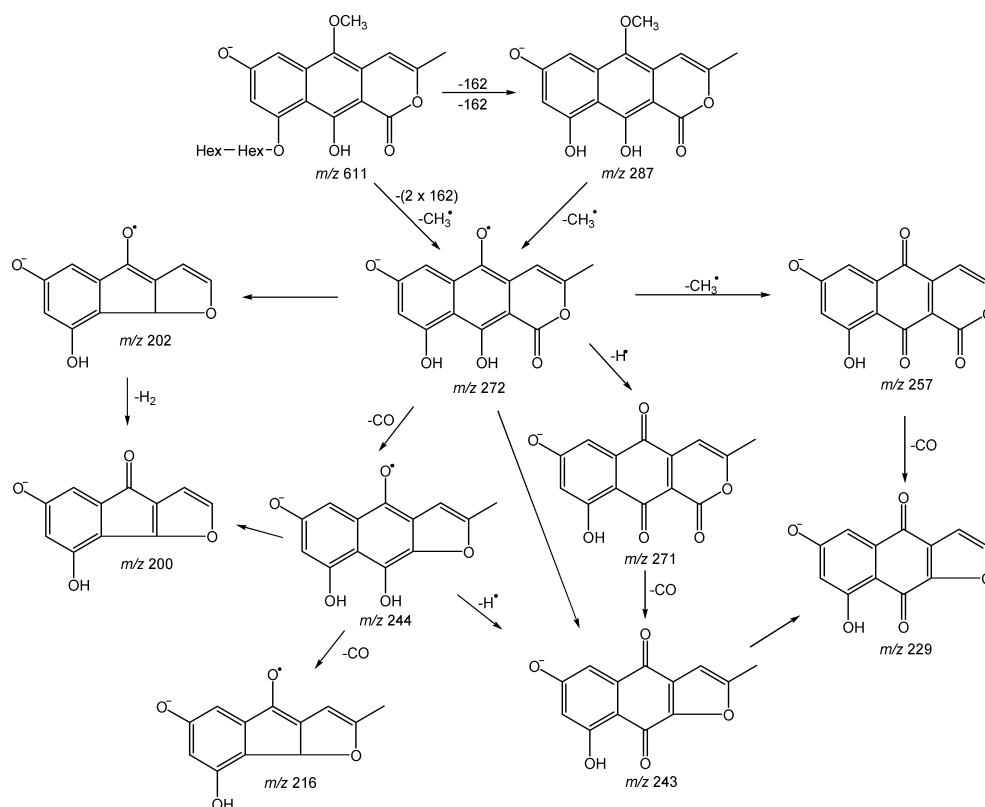


Figure 2. ESIMSⁿ fragmentation pathway of 10.

signals for only one β -glucopyranosyl unit with the anomeric proton at δ 5.15 (d, J = 8.8 Hz) (Table 4). A detailed analysis of NMR data permitted identification of 16 as the new 7,9,10-trihydroxy-5-methoxy-3-methyl-1*H*-naphtho[2,3-*c*]pyran-1-one-9-*O*- β -D-glucopyranoside.

The antioxidant activity of compounds 1–19 was tested by the TEAC assay and expressed as TEAC value, defined as the concentration of Trolox solution with antioxidant potential equivalent to a 1 mM concentration of the test sample.^{15,16} The TEAC values of 1–19 were compared to those of quercetin, quercetin 3-*O*-glucoside, and kaempferol 3-*O*-glucoside (Table 5). The results showed that most flavonoids (1–3, 5–9, 11, 13, 17–19) exhibited higher free-radical-scavenging activity than naphthopyranones (14–16). In particular, flavonoids 2, 6, and 7 were more active than the reference antioxidant compounds, with compound 7 showing the highest antioxidant activity (2.160 mM). The head-to-tail dimer 12 showed antioxidant activity lower than the related flavonoid monomer 18. Among the naphthopyranone compounds, 10 and 16 displayed the highest TEAC values, suggesting that a free hydroxy group at C-7 improves the radical-scavenging capacity.

The ability of several antioxidant plant phenolics to reduce the risk and slow the progression of prostate cancer by prevention of cell oxidation has been widely reported.²⁷

Thus, the cytotoxic activity and the ability of all compounds to affect the levels of intracellular ROS either in the control prostate cancer PC3 cell line or in PC3 cells simultaneously exposed to t-BOOH, a known pro-oxidant, were evaluated. In agreement with TEAC results, the 24 h pretreatment of PC3 cells with 10 μ M 2, 6, and 7, respectively, prevented elevation of ROS induced by t-BuOOH, suggesting the potential activity of these compounds to protect cells from oxidative stress (Figure 3). None of the compounds had a significant cytotoxic

effect on PC3 cancer cells. No significant antioxidant effects were observed with the other analyzed compounds.

EXPERIMENTAL SECTION

General Experimental Procedures. Optical rotations were measured on a JASCO DIP 1000 polarimeter. IR measurements were obtained on a Bruker IFS-48 spectrometer. UV spectra were obtained on a Beckman DU 670 spectrometer. NMR experiments were performed on a Bruker DRX-600 spectrometer at 300 K. All 2D-NMR spectra were acquired in methanol-*d*₄ (99.95%, Sigma-Aldrich), and standard pulse sequences and phase cycling were used for DQF-COSY, HSQC, HMBC, ROESY, and TOCSY spectra. The ROESY spectra were acquired with $t_{\text{mix}} = 400$ ms. Exact masses were measured by an AB SCIEX Voyager DE mass spectrometer equipped with a 337 nm laser and delay extraction and operated in positive ion reflector mode. Samples were analyzed by MALDI-TOF mass spectrometry. A mixture of analyte solution and α -cyano-4-hydroxycinnamic acid (Sigma) was applied to the metallic sample plate and dried. Mass calibration was performed with the ions from adrenocorticotropic hormone (ACTH) fragment 18–39 human at 2465.1989 Da and α -cyano-4-hydroxycinnamic acid at 190.0504 Da as internal standard. The MeOH extract was analyzed by online HPLC-ESIMSⁿ using a ThermoFinnigan Spectra System HPLC coupled with an LCQ Deca ion trap mass spectrometer (ThermoFinnigan, San José, CA, USA). HPLC separation was conducted on a C₁₈ reversed-phase (RP) column (5 μ m, 3 mm \times 150 mm; 100 Å; Luna PFP(2), Phenomenex, Torrance, CA, USA) at a flow rate of 0.2 mL/min. A gradient elution was performed by using H₂O (A) and CH₃CN (B), both added with 0.1% HCO₂H, as mobile phases. After a 3 min hold at 5% B, elution was performed according to the following conditions: from 5% B to 25% B in 8 min; to 26% B in 3 min, hold at 26% B for 10 min; to 27% B in 3 min, hold at 27% B for 5 min; to 38% B in 8 min. The column effluent was analyzed by ESIMS in negative ion mode, and the mass spectra were acquired and processed using the software provided by the manufacturer. The capillary voltage was set at –32 V, the spray voltage at 5 kV, and the tube lens offset at 30 V. The capillary

Table 4. ^{13}C and ^1H NMR Data (J in Hz) of Compounds 10 and 16 (600 MHz, δ ppm, in methanol- d_4)

	10		16	
	δ_{C}	δ_{H} (J in Hz)	δ_{C}	δ_{H} (J in Hz)
1	169.2		169.0	
3	153.4		152.5	
4	99.7	6.62, s	99.5	6.65, s
4a	124.7		124.7	
5	140.2		139.0	
5a	137.2		137.0	
6	99.3	7.06, d (1.5)	99.3	7.07, d (1.5)
7	161.5		160.5	
8	104.7	7.12, d (1.5)	104.7	7.00, d (1.5)
9	160.0		159.0	
9a	110.7		109.6	
10	160.8		160.0	
10a	98.2		97.0	
11	19.3	2.31, s	19.30	2.31, s
OCH ₃ (C5)	61.8	3.85, s	61.5	3.86, s
	β -D-Glc at C-9		β -D-Glc at C-9	
1	103.7	5.03, d (8.8)	104.0	5.15, d (8.8)
2	74.6	3.69, dd (8.8, 9.0)	75.4	3.49, dd (8.8, 9.0)
3	77.1	3.55, dd (9.0, 9.0)	77.1	3.39, dd (9.0, 9.0)
4	71.2	3.47 dd (9.0, 9.0)	71.3	3.25, dd (9.0, 9.0)
5	77.7	3.81 m	77.7	3.44, m
6	69.6	4.24, dd (2.5, 12.0)	68.2	3.86, dd (2.5, 12.0)
		3.89, dd (4.5, 12.0)		3.43, dd (4.5, 12.0)
	β -D-Glc at C-6 _{glc}			
1	104.6	4.48, d (8.8)		
2	74.9	3.31, dd (8.8, 9.0)		
3	77.7	3.27, dd (9.0, 9.0)		
4	71.2	3.34 dd (9.0, 9.0)		
5	77.4	3.39 m		
6	62.4	3.89, dd (2.5, 12.0)		
		3.70, dd (4.5, 12.0)		

temperature was 280 °C. Data were acquired in MS¹ and MSⁿ scanning modes. By using a syringe pump (flow rate 5 $\mu\text{L}/\text{min}$), each pure compound dissolved in MeOH was infused in the ESI source. Negative ESIMSⁿ analyses were performed using the same conditions as those for HPLC-ESIMSⁿ analysis. CC was performed over Sephadex LH-20 (Pharmacia). HPLC-UV separations were performed on an Agilent 1100 series liquid chromatograph, equipped with a G-1312A binary pump, a G-1328B rheodyne injector, and a G-1365B multiple wavelength detector and detecting at $\lambda = 254, 280,$ and 330 nm. GC analysis was performed on a Thermo Finnigan Trace GC apparatus using a I-Chirasil-Val column (0.32 mm \times 25 m). TLC was performed on silica gel F254 (Merck) plates.

Plant Material. Flowers of *P. geniculatus* Kunth. were collected in October 2007 at Santana do Riacho, State Minas Gerais, Brazil, and identified by Professor Paulo Takeo Sano, from the IB-USP. A voucher specimen is deposited at the Herbarium of the Departamento de Botânica do Instituto de Biociências, USP (SPF 139.580).

Extraction and Isolation. Flowers were dried in an oven at 40 °C for a week and powdered. The material (300 g) was extracted by percolation with MeOH (1.5 L) three times for three days, at room temperature. After filtration and evaporation of the solvent to dryness in vacuo, 14.64 g (4.88%) of crude extract was obtained. The dried extract (4.0 g) was dissolved in MeOH (15 mL) and centrifuged for 10 min at 3500 rpm twice. The combined supernatants were fractionated on a Sephadex LH-20 column (56 cm \times 3 cm), using MeOH (1.5 L) as mobile phase, affording 156 fractions (7 mL).

The Sephadex fractions 54–57 (304 mg) and 64–68 (117 mg) were analyzed by HPLC-UV, on a C₁₈ reversed-phase column (Synergi Hydro, 10 μm , 250 mm \times 10.00 mm; 80 Å; Phenomenex, Torrance,

Table 5. Free Radical Scavenging Activities of Compounds 1–19 and the Methanolic Extract of *P. geniculatus* Flowers in the TEAC Assay

compound	TEAC value (mM \pm SD)
1	1.545 \pm 0.075
2	2.017 \pm 0.111
3	1.529 \pm 0.038
4	0.525 \pm 0.025
5	1.373 \pm 0.034
6	2.059 \pm 0.027
7	2.160 \pm 0.031
8	1.267 \pm 0.075
9	1.000 \pm 0.134
10	1.038 \pm 0.017
11	0.968 \pm 0.036
12	0.738 \pm 0.009
13	1.214 \pm 0.015
14	0.706 \pm 0.049
15	0.570 \pm 0.021
16	0.898 \pm 0.030
17	1.397 \pm 0.059
18	1.279 \pm 0.191
19	0.984 \pm 0.041
quercetin	1.866 \pm 0.008
quercetin 3-O-glucoside	1.780 \pm 0.004
kaempferol 3-O-glucoside	1.178 \pm 0.010
	TEAC value (mg/mL \pm SD)
<i>P. geniculatus</i> MeOH extract	1.479 \pm 0.0155

CA, USA), using H₂O + TFA (0.05%) and CH₃CN + TFA (0.05%) as mobile phases, at a flow rate of 2.0 mL/min. Elution was performed according to the following conditions: from 15% B to 25% B in 30 min, hold at 25% B for 20 min; to 35% B in 30 min; to 90% B in 20 min; and to 100% in 10 min.

The chromatographic separation of Sephadex fractions 54–57 yielded 16 compounds: 1 (3.9 mg, $t_{\text{R}} = 22.0$ min), 2 (3.9 mg, $t_{\text{R}} = 25.2$ min), 3 (1.5 mg, $t_{\text{R}} = 27.4$ min), 5 (1.8 mg, $t_{\text{R}} = 28.7$ min), 6 (3.3 mg, $t_{\text{R}} = 30.8$ min), 7 (1.8 mg, $t_{\text{R}} = 33.3$ min), 8 (2.7 mg, $t_{\text{R}} = 33.6$ min), 10 (4.2 mg, $t_{\text{R}} = 36.2$ min), 9 (3.4 mg, $t_{\text{R}} = 37.7$ min), 11 (4.4 mg, $t_{\text{R}} = 39.8$ min), 13 (2.9 mg, $t_{\text{R}} = 43.7$ min), 14 (2.5 mg, $t_{\text{R}} = 47.3$ min), 15 (1.3 mg, $t_{\text{R}} = 51.6$ min), 17 (2.8 mg, $t_{\text{R}} = 56.5$ min), 18 (2.2 mg, $t_{\text{R}} = 68.2$ min), and 19 (1.0 mg, $t_{\text{R}} = 69.6$ min).

The chromatographic separation of Sephadex fractions 64–68 yielded three compounds: 4 (1.6 mg, $t_{\text{R}} = 30.2$ min), 12 (3.5 mg, $t_{\text{R}} = 41.0$ min), and 16 (1.2 mg, $t_{\text{R}} = 54.1$ min).

Compound 1: yellow powder; $[\alpha]_{\text{D}}^{25} -20.3$ (c 0.1, MeOH); UV (MeOH) λ_{max} (log ϵ) 360 (4.20), 260 (4.15) nm; IR (KBr) ν_{max} 3380 (br OH), 2915 (CH), 1680 (C=O), 1656 (C=C), 1618 (C=C), 1580 (C=C), 1460 (C=C) cm^{-1} ; ^1H NMR (methanol- d_4 , 600 MHz) and ^{13}C NMR (methanol- d_4 , 150 MHz) data of the aglycone moiety, see Table 2; ^1H NMR (methanol- d_4 , 600 MHz) and ^{13}C NMR (methanol- d_4 , 150 MHz) data of the sugar portion, see Table 3; ESIMS m/z 639.4 $[\text{M} - \text{H}]^-$; ESIMS/MS (collision energy 30%) m/z 639.1 (57.1), 493.1 (0.3), 457.1 (0.3), 331.1 (100.0), 316.1 (9.3); ESIMS³ (collision energy 32%) of m/z 331.1 (17.3), 316.0 (100.0), 313.0 (7.4), 223.1 (0.7), 209.0 (10.5), 193.0 (0.1), 181.0 (9.8), 166.0 (0.7), 137.4 (0.2); HR-MALDI-TOFMS $[\text{M} + \text{H}]^+$ m/z 641.1716 (calcd for C₂₈H₃₃O₁₇, 641.1712).

Compound 5: yellow powder; $[\alpha]_{\text{D}}^{25} -15.7$ (c 0.15, MeOH); UV (MeOH) λ_{max} (log ϵ) 344 (4.70), 287 (3.85), 217 (4.60) nm; IR (KBr) ν_{max} 3380 (br OH), 2918 (CH), 1676 (C=O), 1660 (C=C), 1615 (C=C), 1570 (C=C), 1456 (C=C) cm^{-1} ; ^1H NMR (methanol- d_4 , 600 MHz) and ^{13}C NMR (methanol- d_4 , 150 MHz) data of the aglycone moiety, see Table 2; ^1H NMR (methanol- d_4 , 600 MHz) and ^{13}C NMR (methanol- d_4 , 150 MHz) data of the sugar portion, see Table 3; ESIMS m/z 681.2 $[\text{M} - \text{H}]^-$; ESIMS/MS

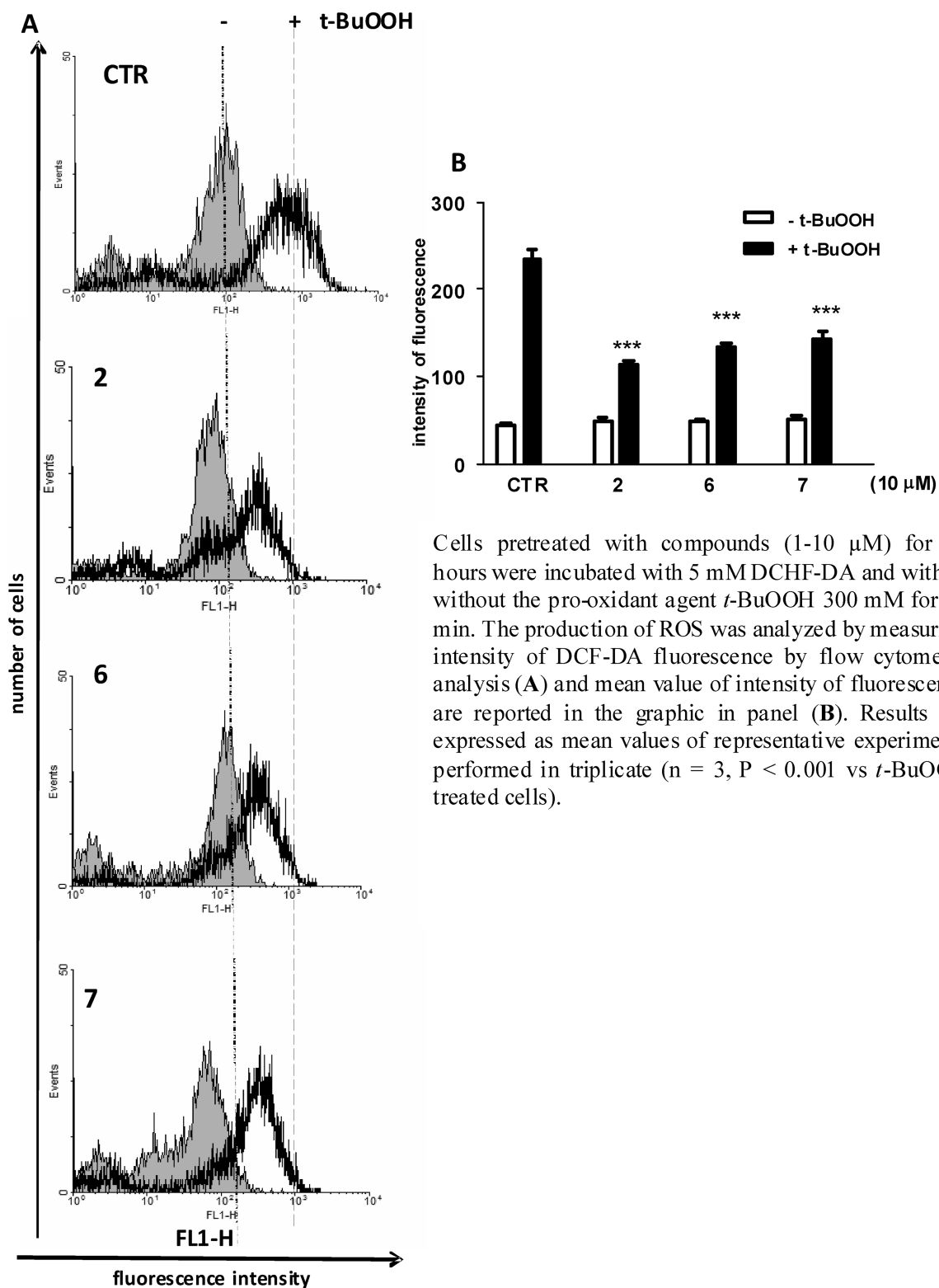


Figure 3. Effects of **2**, **6**, and **7** on ROS production in PC3 cells.

(collision energy 30%) m/z 681.1 (23.4), 639.2 (100.0), 493.1 (1), 331.1 (25.4), 316.0 (2.8); ESIMS³ (collision energy 30%) of m/z 639.1 (100.0), 493.2 (0.2), 457.2 (0.5), 331.1 (77.1), 316.1 (6.6); ESIMS⁴ (collision energy 30%) of m/z 331.1 (43.9), 316.0 (100), 223.0 (2.5), 209.2 (1.2); HR-MALDI-TOFMS $[M + H]^+$ m/z 683.1823 (calcd for $C_{30}H_{35}O_{18}$, 683.1818).

Compound 7: yellow powder; $[\alpha]_D^{25}$ -25.6 (c 0.1, MeOH); UV (MeOH) λ_{max} (log ϵ) 344 (4.72), 285 (3.80), 215 (4.60) nm; IR

(KBr) ν_{max} 3382 (br OH), 2922 (CH), 1684 (C=O), 1658 (C=C), 1618 (C=C), 1578 (C=C), 1460 (C=C) cm^{-1} ; ¹H NMR (methanol- d_4 , 600 MHz) and ¹³C NMR (methanol- d_4 , 150 MHz) data of the aglycone moiety are superimposable with those reported for **5**; ¹H NMR (methanol- d_4 , 600 MHz) and ¹³C NMR (methanol- d_4 , 150 MHz) data of the sugar portion, see Table 2; ESIMS m/z 681.3 $[M - H]^-$; ESIMS/MS (collision energy 30%) m/z 681.1 (11.5), 639.2 (100), 493.1 (1.6), 331.1 (30.3), 316.1 (4.3); ESIMS³ (collision

energy 30%) of m/z 639.1 (51.1), 493.2 (0.4), 457.1 (0.3), 331.1 (100), 316.1 (11.5); ESIMS⁺ (collision energy 30%) of m/z 331.0 (47.9), 316.1 (100), 222.9 (0.4), 209.0 (5.5), 180.9 (3.8); HR-MALDI-TOFMS $[M + H]^+$ m/z 683.1825 (calcd for C₃₀H₃₅O₁₈, 683.1818).

Compound 9: yellow powder; $[\alpha]_D^{25}$ -15.4 (c 0.1, MeOH); UV (MeOH) λ_{max} (log ϵ) 330 (4.70), 285 (3.85), 215 (4.60) nm; IR (KBr) ν_{max} 3380 (br OH), 2918 (CH), 1684 (C=O), 1658 (C=C), 1615 (C=C), 1580 (C=C), 1465 (C=C) cm⁻¹; ¹H NMR (methanol-*d*₄, 600 MHz) and ¹³C NMR (methanol-*d*₄, 150 MHz) data of the aglycone moiety, see Table 2; ¹H NMR (methanol-*d*₄, 600 MHz) and ¹³C NMR (methanol-*d*₄, 150 MHz) data of the sugar portion are superimposable with those reported for **5**; ESIMS m/z 665.2 $[M - H]^-$; ESIMS/MS (collision energy 32%) m/z 665.2 (4.7), 623.1 (50.6), 477.1 (2.4), 315.1 (100.0), 300.0 (25.8); ESIMS³ (collision energy 32%) of m/z 623.1 (3.5), 477.1 (0.1), 315.1 (100.0), 300.1 (25.5); ESIMS³ (collision energy 30%) of m/z 315.1 (5.3), 300.0 (100.0), 195.4 (1.1), 181.1 (0.8), 166.3 (0.1); ESIMS⁴ (collision energy 30%) of m/z 300.0 (0.1), 272.1 (100), 254.1 (9.5), 166.2 (0.4); HR-MALDI-TOFMS $[M + H]^+$ m/z 667.1874 (calcd for C₃₀H₃₅O₁₇, 667.1869).

Compound 10: yellow, amorphous powder; $[\alpha]_D^{25}$ -70.5 (c 0.1, MeOH); UV (MeOH) λ_{max} (log ϵ) 255 (4.60), 279 (4.80), 288 (4.90), 385 (3.88) nm; IR (KBr) ν_{max} 3385 (br OH), 2918 (CH), 1685 (C=O), 1660 (C=C), 1614 (C=C), 1582 (C=C), 1465 (C=C) cm⁻¹; ¹H NMR (methanol-*d*₄, 600 MHz) and ¹³C NMR (methanol-*d*₄, 150 MHz), see Table 4; ESIMS m/z 611.3 $[M - H]^-$; ESIMS/MS (collision energy 30%) m/z 611.2 (0.7), 448.9 (0.4), 287.0 (100.0), 272.1 (47.8); ESIMS³ (collision energy 28%) of m/z 287.1 (0.6); 272.1 (100.0); ESIMS⁴ (collision energy 40%) of m/z 272.2 (40.7), 271.1 (25.9), 257.1 (16.1), 244.1 (30.6), 243.2 (100.0), 229.3 (6.2), 216.1 (38.6), 202.3 (5.5), 200.0 (1.4); ESIMS⁴ (collision energy 38%) of m/z 271.2 (93.9), 243.0 (100.0); ESIMS⁴ (collision energy 38%) of m/z 243.3 (1.5); 229.4 (8.7); ESIMS⁴ (collision energy 30%) of m/z 244.3 (15.4), 243.0 (33.4), 216.1 (13.5), 200.1 (12.7); ESIMS⁴ (collision energy 40%) of m/z 257.1 (5.2), 229.2 (100); ESIMS⁴ (collision energy 40%) of m/z 202.1, 200.1 (26.7); HR-MALDI-TOFMS $[M + H]^+$ m/z 613.1770 (calcd for C₂₇H₃₃O₁₆, 613.1763).

Compound 11: yellow powder; $[\alpha]_D^{25}$ -40.2 (c 0.1, MeOH); UV (MeOH) λ_{max} (log ϵ) 333 (4.70), 287 (3.85), 215 (4.70) nm; IR (KBr) ν_{max} 3376 (br OH), 2920 (CH), 1685 (C=O), 1660 (C=C), 1612 (C=C), 1578 (C=C), 1460 (C=C) cm⁻¹; ¹H NMR (methanol-*d*₄, 600 MHz) and ¹³C NMR (methanol-*d*₄, 150 MHz) data of the aglycone moiety are superimposable with those reported for **9**; ¹H NMR (methanol-*d*₄, 600 MHz) and ¹³C NMR (methanol-*d*₄, 150 MHz) data of the sugar portion are superimposable with those reported for **7**; ESIMS m/z 665.2 $[M - H]^-$; ESIMS/MS (collision energy 30%) m/z 665.2 (15.7), 623.1 (57.1), 477.1 (1.2), 315.1 (100.0), 300.1 (25.1); ESIMS³ (collision energy 30%) of m/z 623.1 (10.1), 477.1 (0.1), 315.0 (100.0), 300.0 (24.0); ESIMS³ (collision energy 30%) of m/z 315.1 (2.4), 300.0 (100.0), 180.9 (0.5); ESIMS⁴ (collision energy 30%) of m/z 300.0 (0.4), 272.1 (100), 165.9 (0.4); HR-MALDI-TOFMS $[M + H]^+$ m/z 667.1876 (calcd for C₃₀H₃₅O₁₇, 667.1869).

Compound 12: white, amorphous powder; $[\alpha]_D^{25}$ -7.4 (c 0.1, MeOH); UV (MeOH) λ_{max} (log ϵ) 355 (4.10), 282 (sh), 265 (3.80) nm; IR (KBr) ν_{max} 3422 (br OH), 1670 (C=O), 1615 (C=C), 1600 (C=C) cm⁻¹; ¹H NMR (methanol-*d*₄, 600 MHz) and ¹³C NMR (methanol-*d*₄, 150 MHz), see Table 1; ESIMS m/z 1247.4 $[M - H]^-$; ESIMS/MS (collision energy 30%) m/z 1247.2 (15.7), 931.1 (100.0), 829.2 (3.3), 623.2 (18.4), 477.0 (1.1); ESIMS³ (collision energy 30%) of m/z 931.0 (5.5), 913.1 (7.4), 829.1 (31.3), 665.1 (8.6), 623.1 (100.0), 477.3 (0.5); ESIMS⁴ (collision energy 30%) of m/z 913.3, 829.1 (100.0), 623.0 (43.0); ESIMS⁴ (collision energy 30%) of m/z 829.1, 785.0 (35.3), 665.1 (100.0), 623.2 (57.8); ESIMS³ (collision energy 30%) of m/z 623.2 (39.8), 477.0 (4.9), 315.1 (100.0), 300.0 (13.9); ESIMS⁴ (collision energy 30%) of m/z 315.1 (50.2), 300.1 (100.0), 180.9 (0.5); ESIMS⁵ (collision energy 30%) of m/z 300.0 (2.6), 272.1 (100.0), 166.9 (5.1); HR-MALDI-TOFMS $[M + H]^+$ m/z 1249.3037 (calcd for C₆₂H₅₇O₂₈, 1249.3031).

Compound 13: yellow powder; $[\alpha]_D^{25}$ -15.8 (c 0.1, MeOH); UV (MeOH) λ_{max} (log ϵ) 335 (4.60), 278 (3.85), 218 (4.60) nm; IR (KBr) ν_{max} 3378 (br OH), 2922 (CH), 1680 (C=O), 1660 (C=C), 1612 (C=C), 1580 (C=C), 1460 (C=C) cm⁻¹; ¹H NMR (methanol-*d*₄, 600 MHz) and ¹³C NMR (methanol-*d*₄, 150 MHz) data of aglycone moiety are superimposable with those reported for **5**; ¹H NMR (methanol-*d*₄, 600 MHz) and ¹³C NMR (methanol-*d*₄, 150 MHz) data of the sugar portion, see Table 3; ESIMS m/z 723.3 $[M - H]^-$; ESIMS/MS (collision energy 30%) m/z 723.1 (5.0), 681.2 (100.0); ESIMS³ (collision energy 30%) of m/z 681.1 (25.1), 639.2 (100.0), 493.0 (1.5), 331.0 (20.6); ESIMS⁴ (collision energy 32%) of m/z 639.2 (18.7), 493.0 (0.1), 331.1 (100.0); ESIMS⁵ (collision energy 32%) of m/z 331.1 (4.7), 223.3 (7.3), 180.9 (8.3); HR-MALDI-TOFMS $[M + H]^+$ m/z 725.1930 (calcd for C₃₂H₃₇O₁₉, 725.1924).

Compound 16: yellow, amorphous powder; $[\alpha]_D^{25}$ -82.3 (c 0.1, MeOH); UV (MeOH) λ_{max} (log ϵ) 256 (4.60), 279 (4.72), 288 (4.80), 385 (3.78) nm; IR (KBr) ν_{max} 3385 (br OH), 2918 (CH), 1685 (C=O), 1662 (C=C), 1617 (C=C), 1581 (C=C), 1465 (C=C) cm⁻¹; ¹H NMR (methanol-*d*₄, 600 MHz) and ¹³C NMR (methanol-*d*₄, 150 MHz), see Table 4; ESIMS m/z 449.2 $[M - H]^-$; ESIMS/MS (collision energy 30%) m/z 449.2 (1.5), 287.0 (100.0), 272.1 (7.9); ESIMS³ (collision energy 30%) of m/z 287.3 (2.4), 272.2 (100.0); ESIMS⁴ (collision energy 40%) of m/z 272.1 (64.9), 271.1 (8.9), 256.9 (3.3), 244.2 (23.6), 243.1 (100.0), 229.0 (7.5), 216.1 (81.5), 202.2 (3.2), 200.3 (10.7); HR-MALDI-TOFMS $[M + H]^+$ m/z 451.1239 (calcd for C₂₁H₂₃O₁₁, 451.1235).

Compound 17: yellow powder; $[\alpha]_D^{25}$ -32.0 (c 0.1, MeOH); UV (MeOH) λ_{max} (log ϵ) 335 (4.70), 288 (3.85), 218 (4.60) nm; IR (KBr) ν_{max} 3380 (br OH), 2929 (CH), 1685 (C=O), 1660 (C=C), 1615 (C=C), 1580 (C=C), 1464 (C=C) cm⁻¹; ¹H NMR (methanol-*d*₄, 600 MHz) and ¹³C NMR (methanol-*d*₄, 150 MHz) data of aglycone moiety are superimposable with those reported for **9**; ¹H NMR (methanol-*d*₄, 600 MHz) and ¹³C NMR (methanol-*d*₄, 150 MHz) data of the sugar portion, see Table 3; ESIMS m/z 707.3 $[M - H]^-$; ESIMS/MS (collision energy 30%) m/z 707.2 (12.6), 665.2 (100.0), 477.1 (4.2), 315.0 (87.5); ESIMS³ (collision energy 30%) of m/z 665.1 (16.2); 623.1 (41.1), 477.3 (1.2), 315.1 (100.0); ESIMS⁴ (collision energy 30%) of m/z 623.1 (9.7), 315.0 (100.0), 300.0 (39.9); ESIMS⁴ (collision energy 30%) of m/z 477.2, 314.9 (6.3), 281.9 (100.0), 181.3 (8.0); ESIMS⁴ (collision energy 30%) of m/z 314.9 (0.8), 300.0 (100.0), 181.1 (1.3); HR-MALDI-TOFMS $[M + H]^+$ m/z 709.1981 (calcd for C₃₂H₃₇O₁₈, 709.1974).

Compound 19: yellow powder; $[\alpha]_D^{25}$ -12.5 (c 0.1, MeOH); UV (MeOH) λ_{max} (log ϵ) 358 (4.10), 280 (sh), 265 (3.80) nm; IR (KBr) ν_{max} 3420 (br OH), 1660 (C=O), 1615 (C=C), 1600 (C=C) cm⁻¹; ¹H NMR (methanol-*d*₄, 600 MHz) and ¹³C NMR (methanol-*d*₄, 150 MHz), see Table 1; ESIMS m/z 653.2 $[M - H]^-$; ESIMS/MS (collision energy 32%) m/z 653.2 (15.0), 477.0 (1.8), 315.1 (100.0); ESIMS³ (collision energy 32%) of m/z 315.1 (26.7), 300.0 (100.0), 181.1 (2.9); ESIMS⁴ (collision energy 32%) of m/z 300.1 (3.9), 272.2 (100.0), 166.1 (8.5); HR-MALDI-TOFMS $[M + H]^+$ m/z 655.1663 (calcd for C₃₂H₃₁O₁₅, 655.1657).

Acid Hydrolysis. The configuration of the sugar units was established after hydrolysis of **1–19** with 1 N HCl, trimethylsilylation, and determination of the retention times by GC operating under the experimental conditions reported by De Marino et al., 2003.²⁸

The peaks of the hydrolysate of **1** were detected at 10.72 (L-rhamnose) and 14.73 min (D-glucose). For the hydrolysate of **10** a peak at 14.73 min (D-glucose) was detected. Retention times for authentic samples after being treated in the same manner with 1-(trimethylsilyl)imidazole in pyridine were detected at 9.67 and 10.70 (L-rhamnose) and 14.71 min (D-glucose).

Antioxidant Activity. Pure compounds were tested by using the TEAC assay.^{17–19} The TEAC value is based on the ability of the antioxidant to scavenge the radical cation 2,2'-azino-bis(3-ethylbenzothiazoline-6-sulfonate) (ABTS^{•+}) with spectrophotometric analysis. The ABTS^{•+} cation radical was produced by the reaction between 7 mM ABTS in H₂O and 2.45 mM potassium persulfate, stored in the dark at room temperature for 12 h. ABTS^{•+} is a blue-green chromogen

with a characteristic absorption at 734 nm. The ABTS^{•+} solution was then diluted with PBS (phosphate-buffered saline, pH 7.4) to an absorbance of 0.70 at 734 nm and equilibrated at 30 °C. Samples were diluted with MeOH to produce solutions of 0.3, 0.5, 1, and 1.5 concentration. The reaction was initiated by the addition of 1 mL of diluted 2,2'-azinobis(3-ethylbenzothiazoline-6-sulfonate) (ABTS) to 10 µL of each sample solution. Determinations were repeated three times for each sample solution. The percentage inhibition of absorbance at 734 nm was calculated for each concentration relative to a blank absorbance (MeOH) and was plotted as a function of concentration of compound or standard, 6-hydroxy-2,5,7,8-tetramethylcroman-2-carboxylic acid (Trolox, Aldrich Chemical Co., Gillingham, Dorset, UK). The percentage inhibition was plotted as a function of compound or standard concentration. The antioxidant activities of MeOH extract and compounds 1–19 are expressed as TEAC values in comparison with TEAC activity of the reported reference compounds, quercetin, quercetin 3-O-glucoside, and kaempferol 3-O-glucoside. The TEAC value is defined as the concentration of standard Trolox solution with the same antioxidant capacity as a 1 mM concentration of the investigated compound. In the case of the extract the TEAC value is defined as the concentration of a standard Trolox solution with the same antioxidant capacity as 1 mg/mL of the tested extract.

Cell Cultures. Human prostate cancer cells (PC3) were cultured in DMEM medium supplemented with 2 mM L-glutamine, 10% heat-inactivated fetal bovine serum, and 1% penicillin/streptomycin (all from Cambrex Bioscience, Verviers, Belgium) at 37 °C in an atmosphere of 95% O₂ and 5% CO₂. Cells were plated at a density of 1 × 10⁵ cells/well (Falcon, BD Bioscience, Bedford, MA, USA) the day before treatment. At the end of the incubation period, the cells were processed for FACS analyses. The cells were used up to a maximum of 10 passages.

Flow Cytometry Estimation of Intracellular Redox State. The effect of the compounds on intracellular reactive oxygen species was evaluated by measuring dichlorofluorescein (DCF) fluorescence. Cells were incubated for 24 h in presence and absence of compounds at different concentrations (1–10 µM). At the end of the incubation time, cells were washed and resuspended (2 × 10⁵ cells/ml) in Hank's balanced salt solution containing 10 µM 2',7'-dichlorodihydrofluorescein diacetate (DCFH-DA). Following a further 20 min incubation at 37 °C, DCF fluorescence was monitored by flow cytometry (FL1-H channel). In order to estimate the antioxidant potential of the compounds, control and treated cells were exposed to 300 µM of the oxidant t-BuOOH for 30 min at 37 °C before DCFH-DA loading.

Statistical Analysis. All the results are shown as mean ± SEM of three experiments performed in triplicate. Statistical comparisons between groups were made using ANOVA followed by the Bonferroni parametric test. Differences were considered significant if *p* < 0.05

■ ASSOCIATED CONTENT

📄 Supporting Information

Spectroscopic and spectrometric data for the new compounds 1, 5, 7, 9–13, 16, 17, and 19. This material is available free of charge via the Internet at <http://pubs.acs.org>.

■ AUTHOR INFORMATION

Corresponding Author

*Tel: +39 089969763. Fax: +39 089969602. E-mail: piacente@unisa.it

Notes

The authors declare no competing financial interest.

■ REFERENCES

- (1) Giulietti, A. M.; Hensold, N. *Acta Bot. Bras.* **1990**, *4*, 133–158.
- (2) Vilegas, W.; Nehmea, C. J.; Dokkedal, A. L.; Piacente, S.; Rastrelli, L.; Pizza, C. *Phytochemistry* **1999**, *51*, 403–409.
- (3) Vilegas, W.; Santos, L. C.; Alécio, A. C.; Pizza, C.; Piacente, S.; De Pauw, E.; Sano, P. T. *Phytochemistry* **1998**, *49*, 207–210.

- (4) Piacente, S.; dos Santos, L. C.; Mahmood, N.; Zampelli, A.; Pizza, C.; Vilegas, W. *J. Nat. Prod.* **2001**, *64*, 680–682.
- (5) Santos, L. C.; Piacente, S.; Pizza, C.; Albert, K.; Dachtler, M.; Vilegas, W. *J. Nat. Prod.* **2001**, *64*, 122–124.
- (6) dos Santos, L. C.; Piacente, S.; Pizza, C.; Toro, R.; Sano, P. T.; Vilegas, W. *Biochem. Syst. Ecol.* **2002**, *30*, 451–456.
- (7) Devienne, K. F.; Raddi, M. S. G.; Varanda, E. A.; Vilegas, W. *Z. Naturforsch., C: J. Biosci.* **2002**, *57*, 85–88.
- (8) Varanda, E. A.; Devienne, K. F.; Raddi, M. S. G.; Furuya, E. M.; Vilegas, W. *Toxicol. in Vitro* **2004**, *18*, 109–114.
- (9) Varanda, E. A.; Varella, S. D.; Rampazo, R. A.; Kitagawa, R. R.; Raddi, M. S. G.; Vilegas, W.; dos Santos, L. C. *Toxicol. in Vitro* **2006**, *20*, 664–668.
- (10) Vilegas, W.; Roque, N. F.; Salatino, A.; Giesbrecht, A. M.; Davino, S. *Phytochemistry* **1990**, *29*, 2299–2301.
- (11) Varanda, E. A.; Raddi, M. S. G.; de Luz Dias, F.; Araújo, M. C. P.; Gibran, S. C. A.; Takahashi, C. S.; Vilegas, W. *Teratogen. Carcinog. Mutat.* **1997**, *17*, 85–95.
- (12) Tavares, D. C.; Varanda, E. A.; Andrade, F. D. P.; Vilegas, W.; Takahashi, C. S. *J. Ethnopharmacol.* **1999**, *68*, 115–120.
- (13) Di Stasi, L. C.; Camuesco, D.; Nieto, A.; Vilegas, W.; Zarzuelo, A.; Galvez, J. *Planta Med.* **2004**, *70*, 315–320.
- (14) Devienne, K. F.; Cálgaro-Helena, A. F.; Dorta, D. J.; Prado, I. M.R.; Raddi, M. S. G.; Vilegas, W.; Uyemura, S. A.; Santos, A. C.; Curti, C. *Phytochemistry* **2007**, *68*, 1075–1080.
- (15) Re, R.; Pellegrini, N.; Proteggente, A.; Pannala, A.; Yang, M.; Rice-Evans, C. *Free Radical Biol. Med.* **1999**, *26*, 1231–1237.
- (16) Piacente, S.; Montoro, P.; Oleszek, W.; Pizza, C. *J. Nat. Prod.* **2004**, *67*, 882–885.
- (17) Thomas, M. B.; Mabry, T. J. *Phytochemistry* **1968**, *7*, 787–790.
- (18) Bonina, F.; Puglia, C.; Ventura, D.; Aquino, R.; Tortora, S.; Sacchi, A.; Saija, A.; Tomaino, A.; Pellegrino, M. L.; de Caprariis, P. *J. Cosmet. Sci.* **2002**, *53*, 321–335.
- (19) Bertrand, C.; Fabre, N.; Moulis, C. *Fitoterapia* **2001**, *72*, 844–847.
- (20) de Andrade, F. D. P.; Rastrelli, L.; Pizza, C.; Sano, P. T.; Vilegas, W. *Biochem. Syst. Ecol.* **2002**, *30*, 275–277.
- (21) de Andrade, F. D. P.; dos Santos, L. C.; Dokkedal, A. L.; Vilegas, W. *Phytochemistry* **1999**, *51*, 411–415.
- (22) Montaudo, G.; Caccamese, S. *J. Org. Chem.* **1973**, *38*, 710–716.
- (23) Ben-Efraim, D. A.; Green, B. S. *Tetrahedron* **1974**, *30*, 2357–2364.
- (24) Chi, Y.-M.; Nakamura, M.; Zhao, X.-Y.; Yoshizawa, T.; Yan, W.-M.; Hashimoto, F.; Kinjo, J.; Nohara, T.; Sakurada, S. *Biol. Pharm. Bull.* **2006**, *29*, 489–493.
- (25) El-Ansari, M. A.; Nawwar, M. A.; Saleh, N. A. M. *Phytochemistry* **1995**, *40*, 1543–1548.
- (26) Isaza, J. H.; Ito, H.; Yoshida, T. *Phytochemistry* **2001**, *58*, 321–327.
- (27) Shukla, S.; Gupta, S. *Nutr. Cancer* **2005**, *53*, 18–32.
- (28) De Marino, S.; Borbone, N.; Iorizzi, M.; Esposito, G.; McClintock, J. B.; Zollo, F. *J. Nat. Prod.* **2003**, *66*, 515–519.